

REFLECTION CORRESPONDENCE FOR EXPOSING PHOTOGRAPH MANIPULATION

Eric Wengrowski

ECE, Rutgers University, Piscataway, NJ 08854

Zhaohui H. Sun, Anthony Hoogs

Kitware Inc., Clifton Park, NY 12065

ABSTRACT

Modern photo editing software enables increasingly realistic image manipulations, through splicing, region copy and paste, and content-aware fill. One potential flaw in manipulations is generating realistic object reflections, such as in bodies of water or glass surfaces. Image reflections involve complicated interactions between lighting, surface materials, and geometry, and they can be very hard to fake. Any inconsistency between the directly observed scene and its corresponding reflection is a strong indication of content manipulation. We propose a novel, physical-level image forensic approach to verify the integrity of reflections through identifying mismatches between objects and their reflections. The proposed algorithm consists of reflection-invariant feature detection and matching, geometric transform estimation, and robust change detection between a scene region and its warped reflection region. This approach complements the large body of digital-level forensic methods, with the advantage of being robust to digital-level image transformations such as compression, blurring, and added noise. Experimental results on authentic and manipulated images demonstrate its efficacy.

1. INTRODUCTION

In an increasingly visual world, the need for image forensics is paramount. Modern photo editing software has allowed artists to make phenomenal, realistic works combining multiple images, but the accessibility of these tools has made malicious photo manipulations more common and convincing too. As realistic, doctored photos have become ubiquitous, public trust in the authenticity of photographs has been eroded.

To address this problem, a number of image forensic techniques have been developed over the years to ensure media integrity [1]. The earlier works focused on digital-level authentication involving image metadata, quantization table, tone scale response, and photo response non-uniformity (PRNU). For a JPEG photograph, one might perform DCT-AC Analysis, Compression Level Analysis (CLA), Color Filter Array (CFA) analysis, Error-level analysis, examine blocking artifacts, high pass filtering, PRNU analysis, or clone detection. However, the majority of these forensic methods can be defeated by simple image operations or re-imaging attacks, such as image capture from projection or

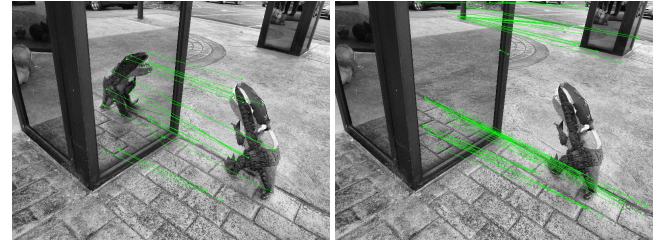


Fig. 1: Left: a dinosaur piñata is matched with its reflection on an outdoor mirror. Right: reflection tampering of editing out the dinosaur reflection has increased errors and removed many of the interest points clustered on the dinosaur’s body.

printing, analog to/from digital conversion, double compression and added noise. Consequently, physical-level forensic methods have been explored to verify the consistency between scene elements, reflection, lighting, and shadows [2, 3]. These methods are robust or invariant to digital-level operations as they involve physical properties of the imaged scene. O’Brien and Farid proposed a human-assisted algorithm for exposing photo manipulation using geometric constraint of reflective vanishing points [2].

Reflections have been studied extensively in image analysis. One primary application is to detect and remove specular highlights using physical models of reflectance [4]. Polarized images were also used to separate reflection components of scenes behind glass [5, 6], taking advantage of the fact that materials like glass will partially polarize light. In addition, reflectance properties have been successfully used for material recognition [7], which could be applicable to matching reflected content by modeling appearance changes from variation in viewpoint and lighting.

In this paper, we study photo integrity using environmental reflections, which contain useful information about the geometry and photometry of objects in a scene. As an example shown in Fig. 1, reliable feature points can be detected and matched on the original image to the left. However, removal of the dinosaur reflection to the right has removed many interest points on the object and increased matching errors. Ersatz reflective geometry might fool the human eye, but image integrity can be verified or questioned if reflective correspondence is known. Because scene reflection involves com-

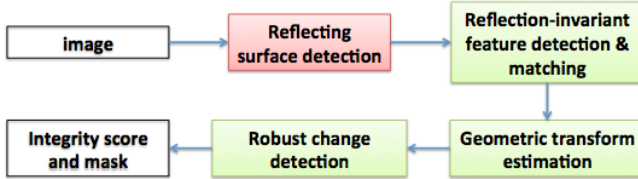


Fig. 2: The work flow of reflection authentication.

plicated interaction between reflecting surface, lighting, and geometry, it is very hard to manipulate an image while maintaining consistent reflection. Therefore the inconsistency between object and its reflection is a good indicator of image tampering, usually stronger than the digital-level forensic indicators. On the other hand, it is challenging to have an end-to-end fully automated solution. Many prior works require human input to manually annotate reflective correspondences, a tedious and error-prone process.

We propose an algorithm for automatically finding point correspondences between scene objects and their reflections, estimating the geometric transform between scene and reflective regions, and detecting inconsistent reflections due to object insertion and removal. The law of reflection is enforced in reflection-invariant feature matching. In addition, the robust change detection module employs a number of heuristics, including the reflected region being compressed in color and contrast and appearing blurry. Rather than requiring matching key points to be explicitly hand-selected by a user, our method requires only a mask of the reflecting region within a single, non-polarized photograph. The proposed algorithm is applicable to photographs that contain specular reflections on planar surfaces, with part of the scene being observed both directly and indirectly through reflection. Planar reflections often appear in nature (e.g. still water surfaces) and are especially common in man-made environments (e.g. mirrors and windows).

The rest of the paper is organized as following. Section 2 outlines the processing pipeline for reflection integrity analysis. Section 3 presents details of each processing module. Experimental results are demonstrated in Section 4, and the paper is concluded in Section 5.

2. REFLECTION INTEGRITY

We first list a few observations to assist our algorithm design.

- The law of reflection. The angle of incidence equals to the angle of reflection, and the incident, normal, and reflected directions are coplanar.
- Compression of color. Object reflection appears less colorful than its direct observation. The color may have shifted. However, the area of color region on color gamut does not increase in reflection.

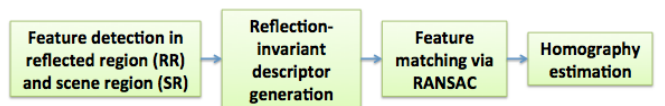


Fig. 3: Reflection-invariant feature matching and geometric transform estimation.

- Compression of sharpness. The reflecting surface serves as a low-pass filter and the reflection usually appears blurrier than directly observed scene.
- Compression of contrast. Due to directional reflection, refraction and surface abortion, only part of the light reaches the sensor after reflection, resulting in lower contrast.

The proposed reflection integrity authentication method follows the processing steps in Fig. 2. The pipeline takes a single image as input. The reflecting surface detection module determines if the image has reflection, and localizes the region of interest. Saliency analysis can further narrow down the sub-region of interest within reflection. Next interest points are identified in scene region (SR) and reflected region (RR). Reflection-invariant feature descriptors are extracted from the feature points and matched across scene and reflection regions. Random sample consensus (RANSAC) is employed to maximize the number of matched features, and the geometric transform and reflection axis are estimated. Upon fixing the geometric transform, the reflection region is warped to the scene region, and robust change detection is carried out. Outliers and anomalies are automatically detected. An integrity score is computed indicating the likelihood of manipulation, and the manipulated region is segmented. The law of reflection is explicitly enforced in feature matching, and compression of color, contrast and sharpness in robust change detection. See Fig. 5 for demonstration of these processing steps.

The first module to detect reflecting surface, highlighted in red in Fig. 2, is out of the scope of this paper, and we manually draw a reflection mask, such as Fig. 5(b). The step can be automated by semantic segmentation [8] or water detection [9]. As shown in Fig. 4, variations in the reflection mask have little effect on the resulting matches. The rest of the pipeline (green) is fully automatic and will be presented in Section 3.

3. PROCESSING MODULES

We first present the algorithm to match the reflected and directly viewed key points within a single image, following the steps in Fig. 3. For a given photograph P , we consider the reflective pixels P_r and the directly imaged pixels P_d . P_r and P_d are computed using a binary mask $M_{\text{reflection}}$ of the reflecting plane R , where $M_{\text{reflection}}(i, j) = 1$ if $P(i, j) \in R$, or $M_{\text{reflection}}(i, j) = 0$ otherwise. Applying $M_{\text{reflection}}$ to P yields the regions of interest, $P_r = M_{\text{reflection}} \wedge P$, and $P_d =$

$\neg(M_{\text{reflection}} \wedge P)$. In other words, P_r and P_d are mutually exclusive, $P_r \cup P_d = P$, and $P_r \cap P_d = 0$.

To better facilitate matching between the two regions, P_r and P_d , we apply the Contrast Limited Adaptive Histogram Equalization (CLAHE) algorithm to both image regions [10, 11], $P'_r = \text{CLAHE}(P_r)$, and $P'_d = \text{CLAHE}(P_d)$.

It is well known many popular feature descriptors, such as SIFT [12] and SURF, are not invariant to affine transforms like reflection. Instead we detect interest point and match the reflection-invariant feature descriptors using [13]. Other alternatives [14, 15, 16, 17] can be used as well. The feature descriptors for both P'_r and P'_d are

$$\begin{aligned} S^r &= \{S_0^r, \dots, S_{m-1}^r\} = \text{Descriptors}(P'_r), \\ S^d &= \{S_0^d, \dots, S_{n-1}^d\} = \text{Descriptors}(P'_d), \end{aligned} \quad (1)$$

where m, n represent the number of computed features in P'_r and P'_d , respectively. Once we have S^r and S^d , our feature-point representations for each image region, we find the correspondences using FLANN (Fast Library of Approximate Nearest Neighbors) [18]. We denote the container F and the total number of matches k such that

$$F_i = \left\{ S_i^{r'}, S_i^{d'} \right\}, \quad \text{where } 0 \leq i \leq k \leq \min(m, n), \quad (2)$$

and $S_i^{r'}, S_i^{d'}$ are the i^{th} feature points matched using FLANN.

For each entry F_i , we calculate the slope L_i of the line segments connecting $S_i^{r'}$ and $S_i^{d'}$. A histogram of all slopes is computed. The number of bins, b , is calculated such that:

$$\begin{aligned} \text{Sturges} &= \log_2 k + 1 \\ \text{FD} &= \frac{\text{IQR}(L)}{\sqrt[3]{k}} \\ b &= \max(\text{Sturges}, \text{FD}), \end{aligned} \quad (3)$$

where $\text{IQR}(L)$ is interquartile range of our slopes L .

Within our histogram, we find the most frequent bin, b^* . Only the interest-point pairs from F in b^* are kept, all others are excluded. We denote this new set of pairs F^* . RANSAC is used to further filter the matched interest-points. The resulting set of matched interest-points is denoted:

$$F^{**} = \{S^{r**}, S^{d**}\}. \quad (4)$$

Given the matched interest points between the scene region and the reflection region, a geometric transform of homography is estimated. We compute the homography H between S^{r**} and S^{d**} from four or more matching points [19]. The estimated transform can then be used to warp the reflection region, and bring the directly-imaged and reflection regions into spatial alignment.

The next step is to locate the outliers and anomalies through robust change detection. Change detection has been long studied. See [20] and references therein for details. However, the images used in the literature tend to be captured

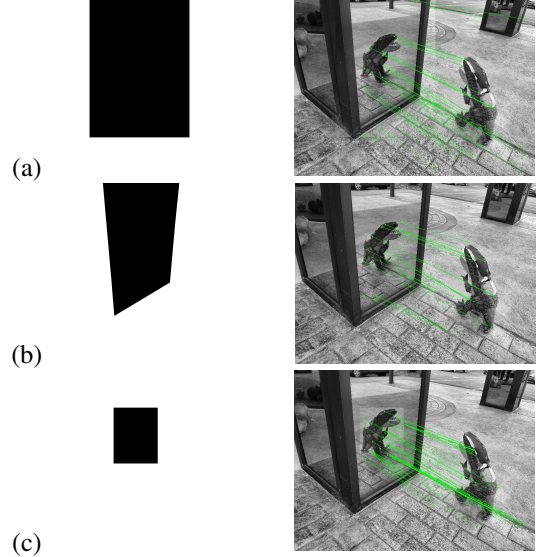


Fig. 4: The reflection matches (right) are robust to perturbations in the reflection mask (left), including the (a) oversized, (b) ground-truth, and (c) undersized reflection masks.

from real cameras. In our case, the scene region is from a real optical camera, and the warped reflection region is from a virtual camera. Various image metrics or similarity measures, such as SSD, MSE, histogram intersection, and disjoint information [21], can be used. The task-specific constraints, such as compression of color, contrast, and sharpness, are used to reduce false detection. To this end, a difference map is calculated from the scene region and the warped reflection region. At each pixel location, a pair of surrounding patches (e.g. 17x17 pixels) are extracted. The standard deviation of the patches are computed. The standard deviation on the reflection patch is subtracted from that on the scene patch, and negative values are truncated to zero. Morphological operations are carried out on the difference map to remove the isolated noise. After thresholding, regions with significant change are identified and an indication score between 0 and 1 is derived from the maximal difference in the region.

4. EXPERIMENTAL RESULTS

In the following, we present the experimental results on authentic and manipulated images with mirror-like reflections.

In Fig. 1, we have an outdoor scene where an object is reflected off the mirrored column of a building. The dinosaur piñata is directly imaged from a very different angle than the reflection. This makes correspondence difficult because few feature points are visible by both viewing angles. The mirror in the scene also introduces some color and intensity bias, making the reflection pixels darker and slightly greener than the directly viewed pixels. Although there are some mismatches corresponding to similarly textured ground bricks

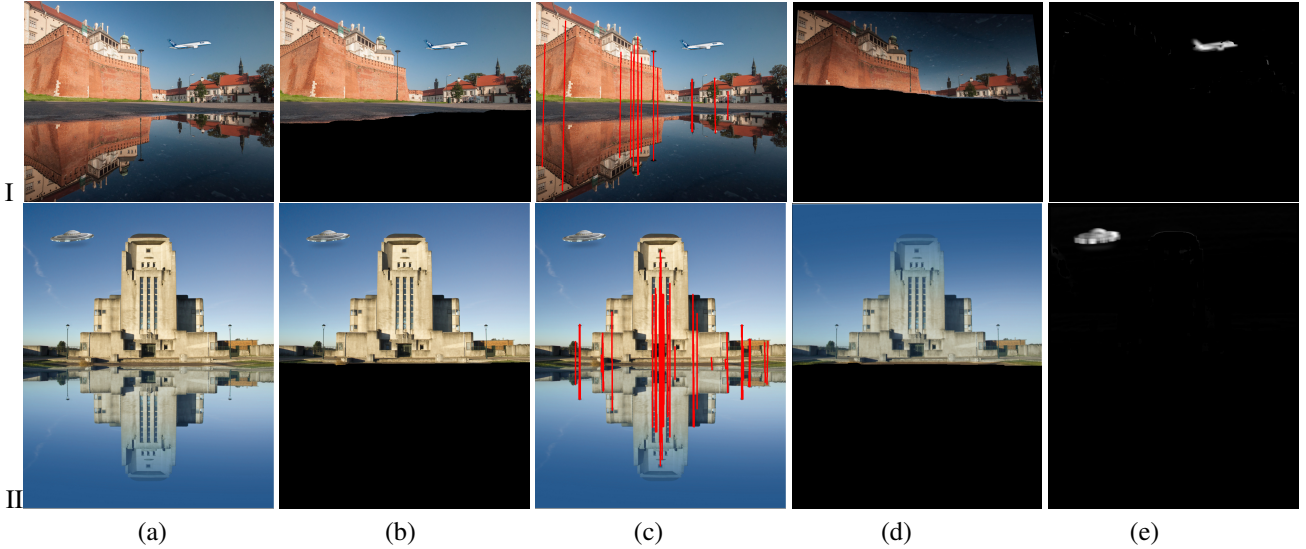


Fig. 5: Photo reflection integrity analysis. (a) Fake images with object insertion of airplane (top) and UFO (bottom). (b) The reflecting surface masks (black regions). (c) Reflection invariant feature matching. (d) The warped reflecting region after applying the estimated geometric transform using correspondence in (c). (e) Robust change detection between (b) and (d).

and mirror frame, this result demonstrates successful reflection matching in a scene with outdoor lighting and where relatively few pixels of the reflection correspond to directly viewed pixels. In the right image, the dinosaur reflection is edited out. The interest-points are no longer clustered on the missing subject. The tampered image has increased matching errors. This is due to a sparsity of similar pixels in the regions, and challenges associated by ambiguous backgrounds.

The proposed feature matching method is robust to the choice of reflection mask. As shown in Fig. 4, even with variable-sized reflection masks, the change in results are minimal. Despite uncontrolled lighting, imperfect reflectors, repeating textures, and occlusions, objects are successfully matched with the proposed method. Our method is not dependent on “perfect results” from an earlier step detecting the reflecting surface plane.

Next we present photo reflection integrity analysis in Fig. 5. Both scene and reflection regions are observable in Fig. 5(a). Note the water in Fig. 5I(a) is actually semi-transparent. The two images are manipulated. An airplane and an UFO are inserted in the sky. However, their reflections are missing. Fig. 5(b) shows the reflection masks, which are drawn manually. Reflection-invariant feature points are detected and matched in Fig. 5(c), as red points and lines. A homography is estimated from the matched points, and the reflection region is warped to the scene region, as shown in Fig. 5(d). Compared to the scene region in Fig. 5(b), the warped reflection regions appear blurrier. There is obvious color shift and contrast reduction. After robust change detection between (b) and (d), the outliers and anomalies are highlighted in Fig. 5(e), which correspond to the image

manipulations.

There is room to improve the robustness of feature matching and change detection. The points in reflection undergo low-pass filtering and geometric warping. In addition, occlusion is prevalent due to the change of viewing angles. Reliable point matching between direct-scene and reflection is still challenging. The reflection surface may have additional content (e.g. stains), and different geometry and photometric properties. Distinguishing manipulation changes versus incidental appearance changes remains a significant challenge.

5. CONCLUSION

We have presented an algorithm to assess photo reflection integrity and expose photo manipulation through reflection correspondence. Feature points are matched between scene region and reflected region. The matching method is robust to general reflection transform and the choice of the reflection mask. Robust change detection is carried out to locate outliers and anomalies, thus revealing inconsistent reflection and photo manipulation. The proposed physical-level forensic indicator complements the widely studied digital-level forensic methods. In the future, we plan to look into automatic reflecting surface detection, and extend the mirror-like planar reflection to other challenging cases.

Acknowledgement This work was supported by AFRL and DARPA under Contract No. FA8750-16-C-0166. Any findings and conclusions or recommendations expressed in this material are solely the responsibility of the authors and do not necessarily represent the official views of AFRL, DARPA, or the U.S. Government.

6. REFERENCES

- [1] Hany Farid, *Photo Forensics*, The MIT Press, 2016.
- [2] James O'Brien and Hany Farid, "Exposing photo manipulation with inconsistent reflections," *ACM Transactions on Graphics*, vol. 31, no. 1, pp. 4, 2012.
- [3] Eric Kee, James F O'Brien, and Hany Farid, "Exposing photo manipulation with inconsistent shadows," *ACM Transactions on Graphics*, vol. 32, no. 3, pp. 28, 2013.
- [4] Shree K Nayar, Xi-Sheng Fang, and Terrance Boult, "Separation of reflection components using color and polarization," *International Journal of Computer Vision*, vol. 21, no. 3, pp. 163–186, 1997.
- [5] Hany Farid and Edward H Adelson, "Separating reflections and lighting using independent components analysis," in *IEEE Conference on Computer Vision and Pattern Recognition*, 1999, vol. 1.
- [6] Naejin Kong, Yu-Wing Tai, and Joseph S Shin, "A physically-based approach to reflection separation: from physical modeling to constrained optimization," *IEEE Trans. on Pattern Analysis and Machine Intelligence*, vol. 36, no. 2, pp. 209–221, 2014.
- [7] Hang Zhang, Kristin Dana, and Ko Nishino, "Reflectance hashing for material recognition," in *IEEE Conference on Computer Vision and Pattern Recognition*, 2015, pp. 3071–3080.
- [8] Evan Shelhamer, Jonathon Long, and Trevor Darrell, "Fully convolutional networks for semantic segmentation," *IEEE transactions on pattern analysis and machine intelligence*, 2016.
- [9] Sheng-Hua Zhong, Yan Liu, Yang Liu, and Chang-Sheng Li, "Water reflection recognition based on motion blur invariant moments in curvelet space," *IEEE Transactions on Image Processing*, vol. 22, no. 11, pp. 4301–4313, 2013.
- [10] Gary Bradski and Adrian Kaehler, *Learning OpenCV*, O'Reilly Meida, Inc., 2008.
- [11] Stephen M Pizer, R Eugene Johnston, James P Erickson, Bonnie C Yankaskas, and Keith E Muller, "Contrast-limited adaptive histogram equalization: speed and effectiveness," in *IEEE Conference on Visualization in Biomedical Computing*, 1990, pp. 337–345.
- [12] David G. Lowe, "Distinctive image features from scale-invariant keypoints," *International Journal of Computer Vision*, vol. 60, no. 2, pp. 91–110, 2004.
- [13] Guoshen Yu and Jean-Michel Morel, "ASIFT: An algorithm for fully affine invariant comparison," *Image Processing On Line*, vol. 1, 2011.
- [14] Xiaojie Guo and Xiaochun Cao, "MIFT: A framework for feature descriptors to be mirror reflection invariant," *Image and Vision Computing*, vol. 30, no. 8, pp. 546–556, 2012.
- [15] Wan-Lei Zhao and Chong-Wah Ngo, "Flip-invariant SIFT for copy and object detection," *IEEE Transactions on Image Processing*, vol. 22, no. 3, pp. 980–991, 2013.
- [16] Asako Kanezaki, Yusuke Mukuta, and Tatsuya Harada, "Mirror reflection invariant HOG descriptors for object detection," in *IEEE International Conference on Image Processing*, 2014, pp. 1594–1598.
- [17] Lingxi Xie, Jingdong Wang, Weiyao Lin, Bo Zhang, and Qi Tian, "RIDE: Reversal invariant descriptor enhancement," in *IEEE International Conference on Computer Vision*, 2015, pp. 100–108.
- [18] Marius Muja and David G. Lowe, "Fast approximate nearest neighbors with automatic algorithm configuration," in *International Conference on Computer Vision Theory and Application*. 2009, pp. 331–340, INSTICC Press.
- [19] R. I. Hartley and A. Zisserman, *Multiple View Geometry in Computer Vision*, Cambridge University Press, second edition, 2004.
- [20] Richard J. Radke, Srinivas Andra, Omar Al-Kofahi, and Badrinath Roysam, "Image change detection algorithms: A systematic survey," *IEEE Transactions on Image Processing*, vol. 14, no. 3, pp. 294–307, March 2005.
- [21] Zhaohui Sun and Anthony Hoogs, "Image comparison by compound disjoint information with applications to perceptual visual quality assessment, image registration and tracking," *International Journal of Computer Vision*, vol. 88, no. 3, pp. 461–488, July 2010.